Available online at www.sciencedirect.com
SCIENCE DIRECT
Thermochimica Acta 438 (2005) 16–21
thermochimica acta
www.elsevier.com/locate/tca

Liquid–liquid interphases at high pressures in presence of compressible fluids

P. Jaeger*, R. Eggers

Process Engineering II, Heat and Mass Transport, Hamburg University of Technology, D-21079 Hamburg, Germany

Received 13 April 2005; received in revised form 21 July 2005; accepted 3 August 2005
Available online 6 September 2005

Abstract

Investigations on phase behaviour and interfacial phenomena in two and three phase fluid systems at pressures up to 250 MPa are presented. The interfacial tension, which is decisive for the energy input for dispersing one fluid phase in the other, was studied as a function of pressure and composition. The effect of pressure on the interfacial tension is generally found to depend on phase behaviour. Partly miscible systems tend to show decreasing interfacial tension as a function of pressure whereas inmiscible liquid–liquid dispersions are hardly affected. In this case, an additional gas phase being mixed with the adjacent liquid phases lowers the interfacial tension to a high extent. At pressures above 100 MPa it becomes increasingly difficult to measure the interfacial tension since the density difference may decrease to extremely low values and pressure induced crystallization may inhibit visualization of the interface. The aim of the presented investigation is to describe interfacial phenomena occurring in liquid–liquid–fluid systems at elevated pressures and quantify the effect of carbon dioxide as a fluid being partly miscible in a number of liquid phases on the interfacial tension.

Keywords: Interfacial tension; High pressure; Pendant drop method; Density

1. Introduction

Interfacial phenomena are decisive in processing of liquid–liquid or liquid–gas systems. Drop sizes, rheology, global hydrodynamics and mass transfer depend not only on bulk phase properties but also on composition, structure and physical characteristics of the interphase like interfacial tension (IFT) and contact angle. Recently, application of elevated pressure is gaining importance implying a tendency towards increasing pressures of up to 100 MPa and more. Some examples are summarized in Table 1.

The behaviour of liquid dispersions was shown to depend on interfacial properties like the interfacial tension [1]. Different authors show that for pure liquid–liquid systems exhibiting little compressibility, the interfacial tension shows an ambiguous behaviour as a function of pressure. Investigations on water–*n*-decane reveal a rise in interfacial tension up to 40 MPa followed by a smooth decline [2]. Other systems of higher mutual affinity show declining interfacial tension like water–carbon dioxide (CO_2) [3]. The course of interfacial tension in gas–liquid systems investigated by Wiegand and Franck [4] depends on molecule size and possibility of interaction of molecules across the interface. The interfacial tension of water–helium increases considerably over the complete investigated pressure range from 0.1 to 250 MPa as a consequence of rebounding forces [5]. Anyway, water–helium is rather an exception with respect to the pressure dependant behaviour of the interfacial tension in liquid–gas systems. Usually, a more or less expressed decline of the interfacial tension is caused by an increasing pressure. In case of high affinity between both adjacent phases and subsequent elevated mutual solubility like in case of oils and CO_2, the interfacial tension decreases dramatically with rising pressure [6]. Above 30 MPa, experimental as well as theoretical work has only been reported on pure systems mainly composed of two components. Vavruch [7] calculates the pressure gradient of the surface tension even

* Corresponding author. Tel.: +49 4 0428782411; fax: +49 4 0428782859.
E-mail address: jaeger@tuhh.de (P. Jaeger).

0040-6031/$ – see front matter © 2005 Elsevier B.V. All rights reserved.
doi:10.1016/j.tca.2005.08.008

Nomenclature

A	interfacial area (m^2)
P	pressure (MPa)
R	gas constant = 8.31451 ($J\,K^{-1}\,mol^{-1}$)
T	temperature (K)
V	volume (m^3)
Greek letters	
Γ	surface excess concentration ($mol\,m^{-1}$)
σ	interfacial tension ($mN\,m^{-1}$)

only of one pure fluid irrespective of practical viability needing a second fluid for pressurization. A number of technical and natural fluid systems contain more than two fluid phases like in oil wells during water flooding in presence of hydrocarbon gases. Beyond its natural appearance, gases can be dissolved in coexisting liquid phases on purpose for creating desired interfacial and rheological properties. Sun and Chen [8] determined interfacial tension of a CO_2–crude oil–water system in order to investigate possibilities of enhanced oil recovery at pressures up to 45 MPa. Up to now, little is known about the interfacial tension in liquid–liquid systems at pressures above 50 MPa. Apart from experimental work presented by Jennings [9] up to 80 MPa, Harvey [10] up to 140 MPa and Wiegand and Franck [4] up to 250 MPa all of them on pure organic substances in contact to water, there is a lack especially in technical relevant systems, e.g. with respect to homogenisation, sterilisation, high pressure freezing, liquid cutting and enhanced oil recovery. Especially here, increased operating pressures are used in order to enhance the kinetic energy, the product yield and to generate specific pressure effects like deactivation of enzymes or a shift in crystallisation temperature. The aim of the present work is to describe interfacial phenomena occurring in liquid–liquid–fluid systems of technical relevance at elevated pressures and quantify the effect of carbon dioxide as a fluid being partly miscible in a number of liquid phases on the interfacial tension.

Table 1
Applications of high pressures

Field	Objective	Pressure (MPa)
Enhanced crude oil recovery	Extension to larger depths	100
High-pressure homogenisation (micro-fluidizer)	Fine, stabilized emulsions	180
High-pressure sterilization	Destroy virus/bacteria	400
High-pressure freezing and subsequent freeze substitution	Obtain cell material without destruction	250
High-pressure water cutting	Transform pressure into kinetic energy	200
Crystallization	Make use of pressure dependent aggregate states	1000

2. Materials

Refined corn germ oil was chosen as the oil phase since former studies were carried out on this system at lower pressures by Jaeger et al. [11] and because of its relevance in food applications like high pressure sterilisation and homogenisation. In order to assure purity with respect to surfactants such as monoglycerides, phospholipids etc. the interfacial tension in distilled water was tested at atmospheric conditions. While interfacial tension of the respective crude corn germ oil from own pressing had a value of 13.7 mN/m at a drop age of 2 s decreasing to 8.5 mN/m after 2 min, interfacial tension of the purified oil amounted to 28.7 mN/m irrespective of drop age which indicates absence of surfactants.

Carbon dioxide of technical purity (99.95%, supplier: Hydrogas) was used. Styrene from BASF AG, Germany had >99% purity and was stabilized with 10 ppm of Butylbrenzcatechine. *n*-Decane (>95%) was supplied by Merck. Methane (>99.5%) and ethane (>99%) were supplied by Westfalen Gas and nitrogen (99.99%) by Linde AG. The water contained an electrical conductivity of about 1 μS and a surface tension of 72 mN/m.

3. Experimental

The liquids and fluids under investigation are contacted within a high-pressure view chamber containing sapphire windows (P_{max} = 400 MPa, D_{window} = 12 mm, V = 6.8 ml). A schematic diagram of the experimental set-up is presented in Fig. 1. By use of hand, piston pumps SP1 to SP3, the fluids and liquids under investigation are metered into the view chamber. SP1 and SP3 had a maximum volume of 7.5 ml while the volume of SP2 (CO_2 supply) amounted to 18 ml. Pressure was determined by pressure transducers (WIKA) at ±0.1 MPa accuracy. The temperature was measured by a thermocouple within the view chamber to an accuracy of ±0.3. The liquid of highest density is passed through a capillary entering the chamber from the top until a pendant drop is generated at its tip within the surrounding liquid/fluid phase. The shape of this drop depends on the interfacial tension and on the densities of the adjacent fluid phases [11]. According to the Laplace equation of curved fluid surfaces, the interfacial tension is determined from digitalized drop images taken by a CCD-camera and using a computer algorithm developed by Song and Springer [12]. Measurements of interfacial tension where repeated evaluating at least three different drop shapes.

One drawback of applying the pendant drop technique is the need of determining the actual densities of the participating fluid phases in order to obtain reliable data. Assuming non-miscibility in water–oil systems, density data may be retrieved from literature [13], [14]. Density of oil saturated with carbon dioxide (CO_2) was investigated by Tegetmeier et al. [15] at pressures up to 35 MPa. Above 150 MPa, only data of pure substances like water and CO_2 are available

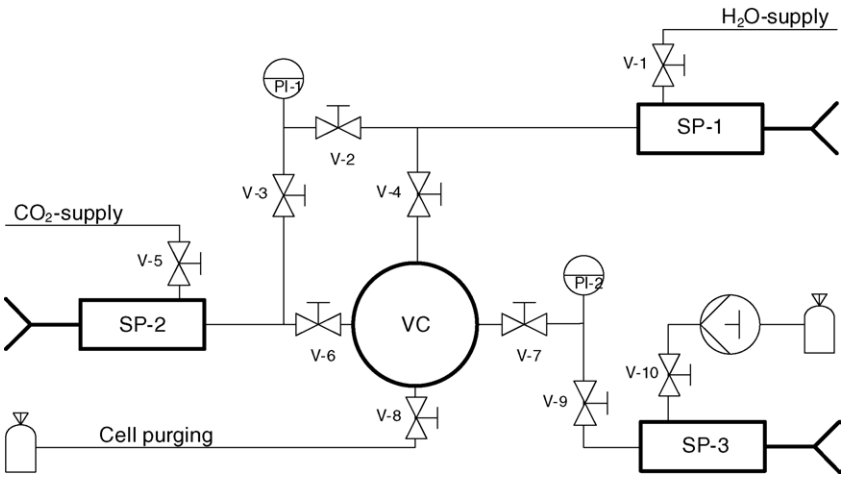

Fig. 1. Experimental set-up for determining the interfacial tension at pressures >100 MPa, SP1 to SP3: hand piston pumps, VC: view chamber.

[16]. At higher pressures, the density of a triglyceride oil was determined by Eder et al. [17] up to 400 MPa using an interferometric method. In the lower pressure region, these data coincide quite well with data of Acosta et al. [14]. Own density data especially of oil containing dissolved CO_2 were obtained by the mass–volume method: a sample was collected in a sample trap of exactly known volume from where both fluids were collected separately after controlled depressurization. Next to the mixture density, the mass fraction of CO_2 is determined by this method. Experimental uncertainty is quite high, but in contrast to the interferometric method, it is possible to work at higher CO_2-contents of up to saturation concentrations. As a consequence, an important source of the error in measurement is reliability of the density data. Considering also image quality and variance within the evaluation procedure, the general accuracy in the interfacial tension measurements was in the range of ±2–3%.

4. Results

Fig. 2 shows images of water drops in triglyceride oil at pressures up to 250 MPa. At about 250 MPa and 20° C the surrounding oil phase becomes opac-impeding detection of the drop shape. Decreasing the pressure leads again to a transparent oil phase. Hence, determination of the interfacial tension by the pendant drop method was limited to pressures of 250 MPa.

4.1. Interfacial tension in water–oil

Fig. 3 shows the interfacial tension of a water drop in corn germ oil as a function of the pressure. These data were obtained, using water density of [16] and oil density of Eder et al. [17]. The resulting interfacial tension shows a slightly rising course until arriving at almost constant values above 150 MPa.

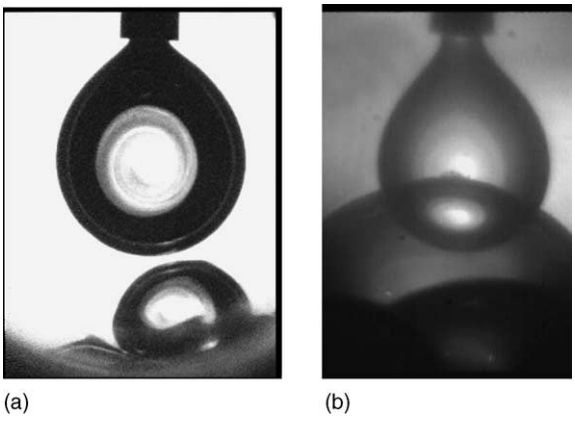

Fig. 2. Water drops in refined corn germ oil at 293 K and (a) 200 MPa, (b) 250 MPa.

4.2. Influence of compressed CO_2 on the water–oil interface

In order to investigate the influence of carbon dioxide as a third fluid phase, the chamber was first filled with this fluid at

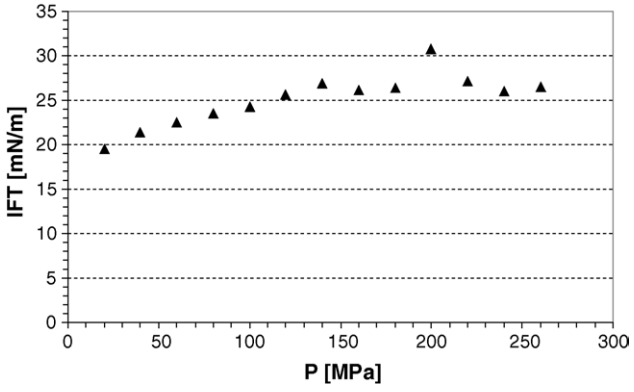

Fig. 3. Interfacial tension of water in triglyceride oil as a function of pressure at 293 K.

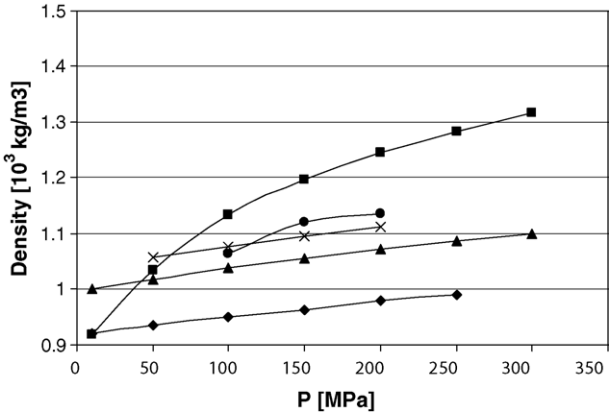

Fig. 4. Density of triglyceride oils in presence of CO_2: comparison to pure liquids, 293 K. (♦) Sunflower oil [13]; (■) CO_2 [12]; (×) oil + 30 wt.% CO_2 [13]; (▲) water [9]; (●) present data: corn germ oil + 30 wt.% CO_2.

conditions corresponding to the designated concentration in the oil phase. Afterwards oil was added up to the desired pressure. During generation of the water drop, a small amount of the surrounding fluid mixture (oil + CO_2) was retrieved into a sample trap from which the amount of oil and CO_2 may be determined after decompression. Fig. 4 shows the density of oil–CO_2 mixtures determined by different methods compared to the pure phase densities of the liquids under investigation. At pressures above 100 MPa, the equilibrium concentration of CO_2 in the oil phase rises clearly above 30%. Under these conditions, own experimental data as well as interpolated data from literature show that the oil + CO_2 density rises above the water density. Both densities approach each other when rising the CO_2-content up to a certain value resulting in almost spherical drops and consequently complicating determination of the interfacial tension. Consequently, measurements regarding the influence of CO_2 on the interfacial tension were carried out first using small amounts of CO_2 being completely dissolved in the oil phase. Fig. 5 shows the influence of the CO_2-concentration on the interfacial tension

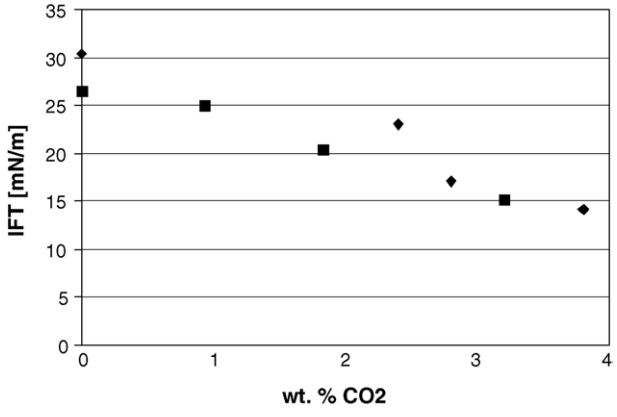

Fig. 5. Interfacial tension of water in corn germ oil containing dissolved CO_2 at 293 K. (■) 150 MPa; (♦) 200 MPa.

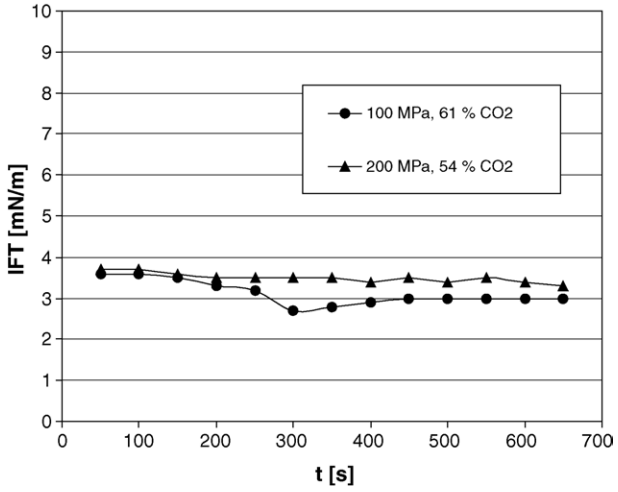

Fig. 6. Interfacial tension of water in corn germ oil/CO_2 as a function of time at 293 K. (▲) 100 MPa, 61 wt.% CO_2; (■) 150 MPa, 56 wt.% CO_2; (♦) 200 MPa, 54 wt.% CO_2.

up to 4 wt.% of CO_2. The interfacial tension was found to depend on the CO_2 concentration rather than on pressure.

In a second step, the amount of CO_2 within the oil phase was increased to a higher extent but still maintaining a concentration below saturation avoiding formation of a third fluid phase. Since the water is not presaturated before the drop comes into contact with the oil + CO_2 phase, the effect of mass transfer, i.e. drop age on interfacial tension should be considered. Nevertheless, results shown in Fig. 6 indicate that the equilibrium value of the interfacial tension is reached fairly fast as a result of a rapid achievement of the equilibrium composition within the interphase. Random-like variations are mostly due to poor image quality since the conditions are near saturation of CO_2 and the surrounding phase is slightly turbid. In general, the obtained values are near 20% of the interfacial tension of the pure oil–water system.

The absolute amount of CO_2 entering the water drop could not be analysed directly. According to Tödheide and Franck [18] near 8–9 wt.% of CO_2 enter the water phase at 100 MPa once equilibrium is established. Thus, generated drop volumes of near 80 μl result in an uptake of 8.5 mg of CO_2. This means a decrease of near 1 wt.% with respect to the surrounding oil/CO_2 phase ($V_{chamber}$ = 6.8 ml) assuming a mixture density of 1.1 g/ml. Compared to the amount of dissolved CO_2 this change seems negligible.

4.3. Fat crystals at elevated pressure

As stated before, the surrounding oil phase becomes opac at very high pressure, which is due to pressure-induced crystallisation. Fat crystals play an important role in emulsion technology since they inhibit coalescence of water drops in a continuous oil phase and consequently stabilize water in oil emulsions [19]. The water drops generated in this work were also perfectly stabilized as long as pressure was main-

Table 2
Composition of different oils, product specifications from Bellmer, Germany

Oil	Saturated (%)	Single-unsaturated (%)	Poly-unsaturated (%)
Corn germ oil	12	29	59
Sunflower oil	11	27	62
Palm oil	53	37	10
Soybean	9	26	65

tained above 220 MPa. After pressure reduction to 180 MPa, coalescence of the accumulated drops sets on, resulting in a continuous water phase at the bottom of the chamber.

Corn germ oil and sunflower oil used for the experiments contain a similar triglyceride spectrum with respect to the grade of saturation of the fatty acids (Table 2).

At 20° C both, corn germ and sunflower oil start to form fat crystals between 235 and 240 MPa whereas palm oil is solid at ambient pressure. This pressure dependent behaviour of crystal formation is attributed to their specific volume, which is smaller than the liquid triglycerides as presented by Lopez et al. [20]. In case of milk fat, it was found that the solid density is about 4% higher than the liquid phase density. Triglycerides usually take α, β and β′ crystal modifications. By pressure treatment formation of β is favoured since it contains the lowest specific volume and the highest melting point. In presence of carbon dioxide crystallisation is initialized at lower pressures. Fig. 7 shows a water drop in an oil–CO_2 mixture were a turbid layer is formed at the bottom of the chamber already at 200 MPa. This shift in crystallisation point may be due to a change in liquid–solid phase equilibria associated also to a change in mixture density. On the other hand, gas clusters may promote nucleation already at lower pressures preventing over-saturation of pure liquid phase systems. The crystals start forming at the bottom because of their higher density. At pressures above 200 MPa it was not possible to visualize drops because of turbidity of the complete surrounding oil + CO_2 phase.

Fig. 7. Water drop in corn germ oil containing CO_2, 200 MPa, 293 K. The turbid front at the bottom influences the drop shape.

5. Discussion

In general, the interfacial tension of the oil–water system is in the range of purified edible oil–water systems [21] having eliminated all surface-active substances. The influence of pressure on the interfacial tension in the water–oil system is typical as found in case of immiscible liquids. From the partial differential of the Gibbs free energy with respect to the area and to the pressure follows the well-known equation relating the pressure gradient of the interfacial tension to the change in volume at changing interfacial area [22]:

$$\left(\frac{\partial\sigma}{\partial P}\right)_{T,A,n} = \left(\frac{\partial V}{\partial A}\right)_{T,P,n} \quad (1)$$

According to the density gradient theory revealed by Turkevich and Mann [23], this pressure coefficient of the interfacial tension may be interpreted as a width being proportional to the thickness of the interfacial layer. Following this idea, there is an increase in volume at the interphase in case of repulsion of the adjacent phases as stated by Motomura et al. [24]. The respective molecules at the interface take more space as in the bulk phase leading to an increasing volume when increasing the interfacial area while maintaining constant pressure. The specific change in volume (right hand side of Eq. (1)) may also be expressed by the amount of molecules leaving the bulk phase by adsorbing at the interface from which the increase in intrinsic volume of the interface, Δv_σ, is subtracted:

$$\left(\frac{\partial\sigma}{\partial P}\right)_{T,A} = -\sum \frac{\Gamma kT}{P} + \Delta v_\sigma \quad (2)$$

Neglecting the volume of the molecule layer at the interface leads to the Gibbs-like equation for relating the change in interfacial tension to the adsorption [5]:

$$\Gamma_{\mathrm{fl}} = -\frac{P}{RT}\left(\frac{\partial\sigma}{\partial P}\right)_T \quad (3)$$

Molecules at the water–oil interface take more space as bulk molecules leading to a negative excess concentration, which is related to a rise of the interfacial tension as a function of pressure below 100 MPa. Depending on the molar volume of a third component at the interface there is a changing influence of pressure on its surface activity. In order to determine the effect of this component on the pressure coefficient in a two phase system Horváth-Szabó et al. [25] used the concept of the so-called conditional relative surface excess (CRSE): the difference in surface excess volume densities between a two phase system containing surfactant and a reference system without surfactant each being described by its specific pressure coefficient (left hand side of Eq. (2)), leads to the actual molar volume of the surfactant at the interface. Transferred to an oil–water system containing CO_2 as a possible surface-active agent, this would mean that the difference in pressure coefficient compared to the pure oil–water system is related to the surface activity of carbon dioxide. Comparing Fig. 4 to Fig. 6 reveals that in both cases, the pressure

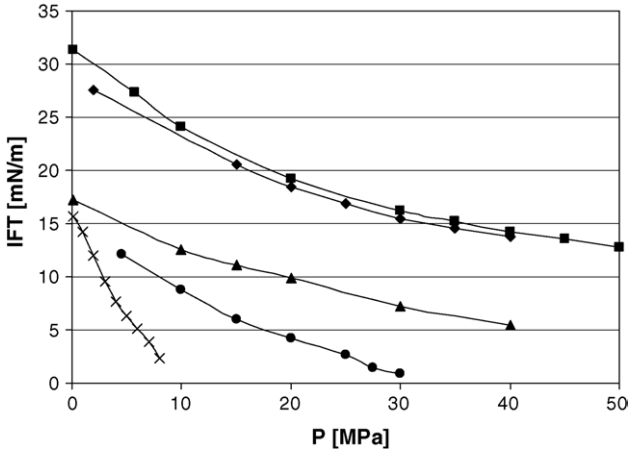

Fig. 8. Interfacial tension as a function of pressure in liquid–gas systems. (♦) N_2–styrene, 296 K; (■) N_2–gasoil, 296 K; (▲) N_2–*n*-decane, 398 K; (●) methane–*n*-decane, 398 K; (×) ethane–*n*-decane, 398 K.

coefficient takes values close to zero. Only the concentration of carbon dioxide itself takes influence on the interfacial tension. Sun and Chen [8] also find, that at low CO_2 concentrations the slope of the interfacial tension is hardly affected while the absolute value clearly decreases at increasing CO_2 concentration.

Turkevich and Mann [23] conclude that the pressure effect on the interfacial tension is composed of the rather smaller thermodynamic effect discussed above and a larger effect by the behaviour of the bulk phases. In case of a gas being strongly miscible in the adjacent liquid phases this becomes clear from the results presented in Fig. 8 using the set-up from Fig. 1 only with SP1 to generate the liquid drop and SP2 for establishing the desired gas/fluid pressure: the interfacial tension reflects the phase behaviour of the bulk system. Close to the critical point of a two phase system, a linear slope of the interfacial tension may be observed until the interface disappears at the transition to the single phase region as shown, e.g. in case of mixtures containing methane and ethane. This behaviour has also been described by Jaeger et al. [6] in systems containing styrene in a carbon dioxide atmosphere.

6. Conclusions

Interfacial tension in inmiscible liquid–liquid systems does not depend much on pressure whereas presence of a gas like carbon dioxide dissolved in one of two adjacent liquid phases results in a considerable decrease. At the same time the density of the oil + CO_2 phase is enhanced as a result of the higher density of carbon dioxide at the respective pressure. In this way, density of the water and the oil-rich phases take similar values resulting in nearly spherical drops. Anyway, above 230 MPa fat crystals are formed that impede visual detection of drops within the oil phase and stabilize water drops against coalescing. In presence of a dissolved gas like carbon dioxide, formation of fat crystals take place at lower pressures as a consequence of shifted phase equilibria and earlier nucleation. In terms of emulsification especially using high-pressure homogenizers, this fact implies possibilities of innovative processes aiming for new product properties and optimizing energy consumption.

Acknowledgement

This work was financed by the German foundation “Deutsche Forschungsgemeinschaft, DFG” under Eg 72/17.

References

[1] J.J.M. Janssen, A. Boon, W.G.M. Agterof, AIChE J. 40 (1994) 1929.
[2] A.S. Michaelis, E.A. Hauser, J. Phys. Chem. 55 (1951) 408.
[3] E.W. Hough, G.J. Heuer, J.W. Walker, Petrol. Trans., AIME 216 (1959) 469.
[4] G. Wiegand, E.U. Franck, Ber. Bunsenges. Phys. Chem. 98 (1994) 809.
[5] A.I. Rusanov, Phasengleichgewichte und Grenzflächenerscheinungen, Akademie Verlag, Berlin, 1978, 99 pp.
[6] Ph.T. Jaeger, R. Eggers, H. Baumgartl, J. Supercrit. Fluids 24 (2002) 203.
[7] I. Vavruch, Langmuir 11 (1995) 2843.
[8] C.-Y. Sun, G.-J. Chen, J. Chem. Eng. Data 50 (2005) 936.
[9] H.Y. Jennings, J. Colloid Interface Sci. 24 (1967) 323.
[10] R.R. Harvey, J. Phys. Chem. 62 (1958) 322.
[11] Ph.T. Jaeger, J.V. Schnitzler, R. Eggers, Chem. Eng. Technol. 19 (1996) 197.
[12] B. Song, J. Springer, J. Colloid Interface Sci. 184 (1996) 64.
[13] National Institute of Standards (NIST), Properties of pure fluids database, http://webbook.nist.gov/chemistry/fluid.
[14] G.M. Acosta, R.L. Smith, K. Arai, J. Chem. Eng. Data 41 (1996) 961.
[15] A. Tegetmeier, D. Dittmar, A. Fredenhagen, R. Eggers, Chem. Eng. Proc. 39 (2000) 399.
[16] R. Span, W. Wagner, J. Phys. Chem. Reference Data 25 (1996) 1509.
[17] C. Eder, A. Delgado, M. Golbach, R. Eggers, 11. Fachtagung zu Lasermethoden in der Strömungsmesstechnik 9–11.9.2003, pp. 28.1–28.6.
[18] K. Tödheide, E.U. Franck, Z. Phys. Chem., Neue Folge 37 (1963) 388.
[19] F. Groeneweg, F.V. Voorst Vader, W.G.M. Agterof, Chem. Eng. Sci. 48 (1993) 229.
[20] C. Lopez, C. Bourgaux, P. Lesieur, M. Ollivon, Lait 82 (2002) 317.
[21] C.C. Ho, M.C. Chow, JAOCS 77 (2000) 191.
[22] M. Kahlweit, Ber. Bunsenges. Phys. Chem. 74 (1970) 636.
[23] L.A. Turkevich, J.A. Mann, Langmuir 6 (1990) 445.
[24] K. Motomura, H. Iyota, M. Aratono, M. Yamanaka, R. Matuura, J. Colloid Interface Sci. 93 (1983) 264.
[25] G. Horváth-Szabó, H. Høiland, K. Martinás, J.A.W. Elliott, J. Dispersion Sci. Techol. 24 (2003) 185.